Electronic Supplementary Material (ESI) for Dalton Transactions.

Light-Initiated Reversible Conversion of Macrocyclic Endoperoxides Derived from Half-Sandwich Rhodium-Based Metallarectangles

Wei-Long Shan, Wen-Xi Gao, Yue-Jian Lin and Guo-Xin Jin*

State Key Laboratory of Molecular Engineering of Polymers, Collaborative Innovation Center of Chemistry for Energy Materials, Department of Chemistry, Fudan University,
Shanghai 200433, P. R. China.

*E-mail: gxjin@fudan.edu.cn.

Contents

1. Synthesis of binuclear complex

A Ag(OTf) (51.4 mg, 0.2 mmol) was added to a solution of $[Cp^*RhCl_2]_2$[1] (31.0 mg, 0.05 mmol) in CH_3OH (10 mL) at room temperature. The mixture was sheltered from light and stirred for 3 h, followed by filtration to remove AgCl, and at which point the BP4VA ligand (19.3 mg, 0.05 mmol) was added to the filtrate. The mixture was then stirred at room temperature for 12 h. The solvent was then concentrated to about 3 mL. Upon the addition of diethyl ether, a red solid of the binuclear complex precipitated and was collected and dried under vacuum after washing with diethyl ether. Yield: 60 mg, 82%. Data for *binuclear complex*: ^{1}H NMR (400 MHz, CD_3CN, ppm): δ = 1.70 (s, 30H, Cp*-H), 7.13 (d, J = 16.4 Hz, 2H, -CH=CH-), 7.61 (dd, J = 6.8, 3.6 Hz, 4H, anthracene-H), 8.00 (d, J = 6.4 Hz, 4H, pyridyl-H), 8.41 (dd, J = 6.8, 3.2 Hz, 4H, anthracene-H), 8.57 (d, J = 16.4 Hz, 2H, -CH=CH-), 8.63 (d, J = 6.4 Hz, 4H, pyridyl-H). IR (KBr disk, cm^{-1}): ν = 3473 (s), 2320 (w), 1610 (m), 1458 (w), 1429 (w), 1381 (w), 1279 (s), 1258 (s), 1225 (w), 1162 (m), 1066 (w), 1031 (s), 845 (w), 762 (w), 639 (m), 577 (w), 518 (w), 449 (w).

References

1 C. White, A. Yates and P. M. Maitlis, *Inorg. Synth.,* 1992, **29**, 228.

2. Crystal Structure

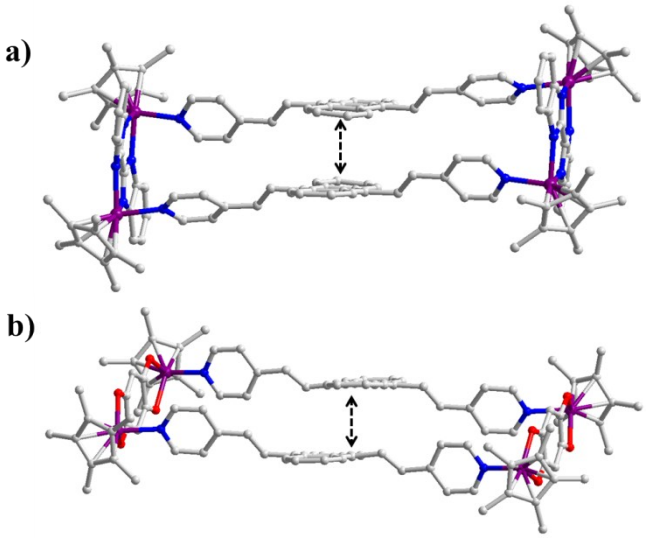

Figure S1. (a) The intramolecular π…π interaction in **5**; (b) The intramolecular π…π interaction in **6**. All hydrogen atoms, solvent molecules, and counterions are omitted for clarity. Color code: N, blue; O, red; C, gray; Rh, purple.

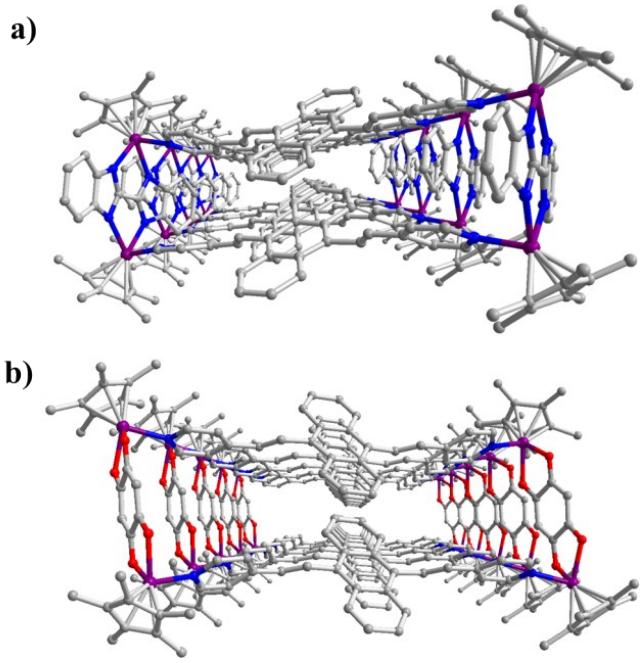

Figure S2. (a) Stacking of the molecules in crystals of **5** viewed along the *y* axis; (b) Stacking of the molecules in crystals of **6** viewed along the *y* axis. All hydrogen atoms, solvent molecules, and counterions are omitted for clarity. Color code: N, blue; O, red; C, gray; Rh, purple.

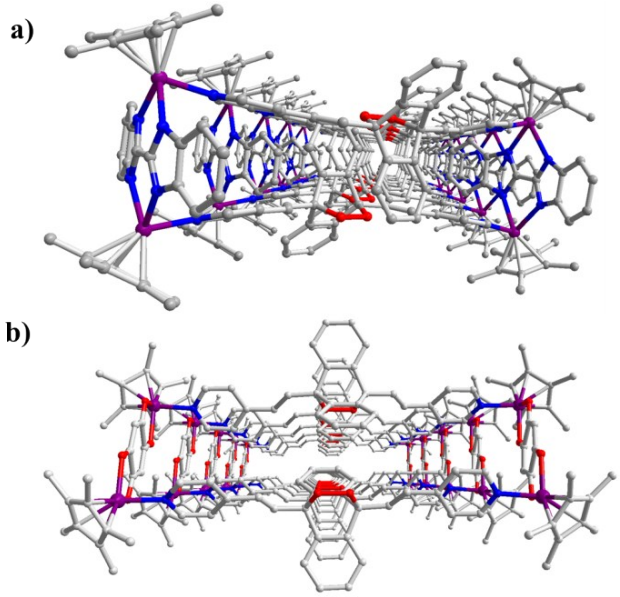

Figure S3. (a) Stacking of the molecules in crystals of **5-O_2** viewed along the *y* axis; (b) Stacking of the molecules in crystals of **6-O_2** viewed along the *y* axis. All hydrogen atoms, solvent molecules, and counterions are omitted for clarity. Color code: N, blue; O, red; C, gray; Rh, purple.

3. NMR Spectra

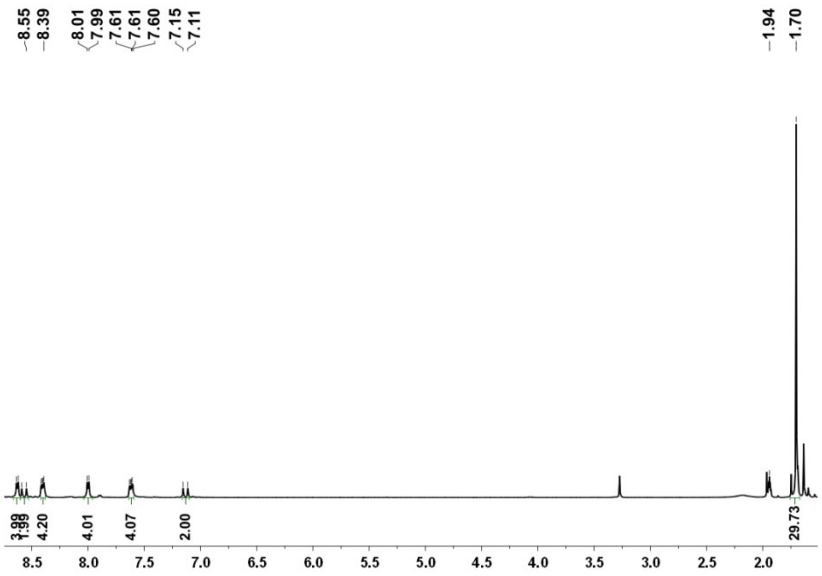

Figure S4. ^{1}H NMR (400 MHz, CD_3CN, ppm) for the binuclear complex.

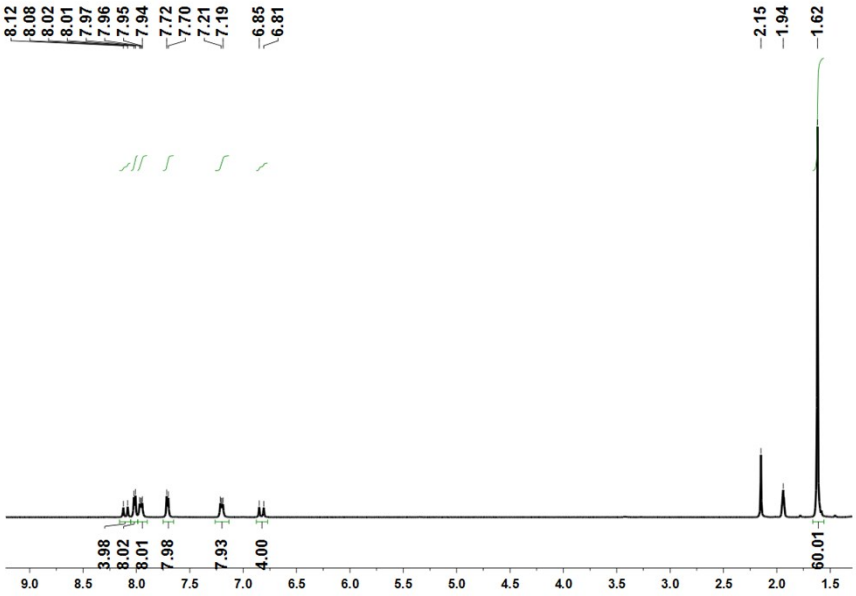

Figure S5. ^{1}H NMR (400 MHz, CD_3CN, ppm) for complex **4**.

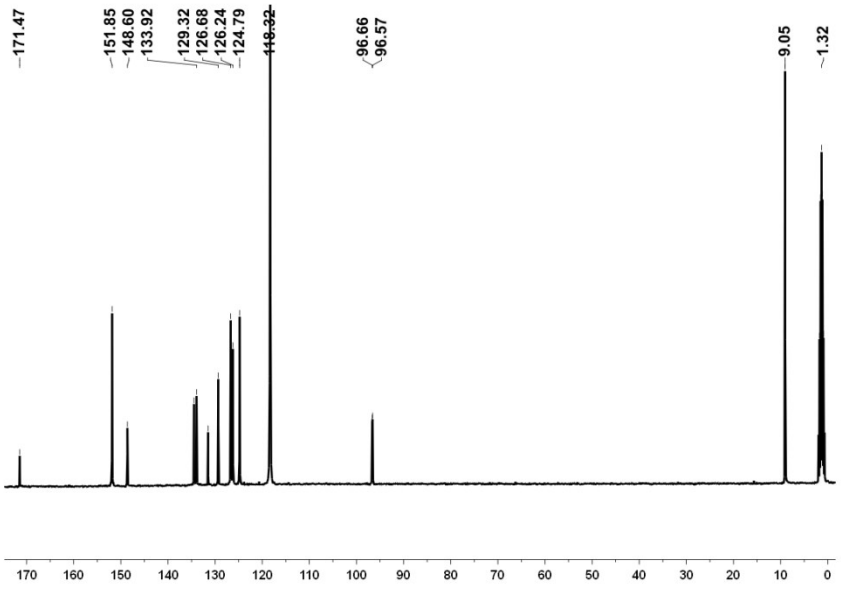

Figure S6. $^{13}C\{^{1}H\}$ NMR (101 MHz, CD_3CN, ppm) for complex **4**.

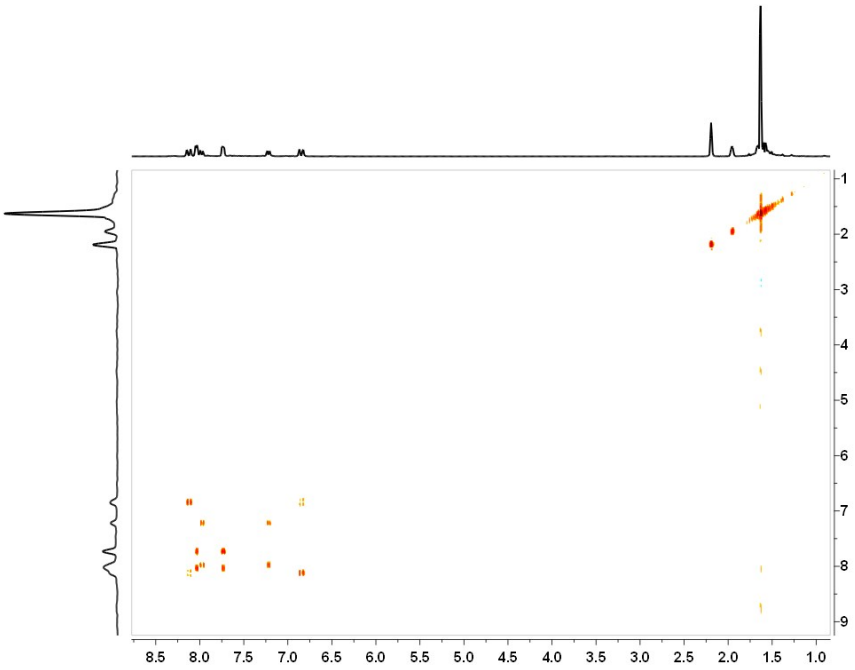

Figure S7. ^{1}H-^{1}H COSY NMR (400 MHz, CD_3CN, ppm) for complex **4**.

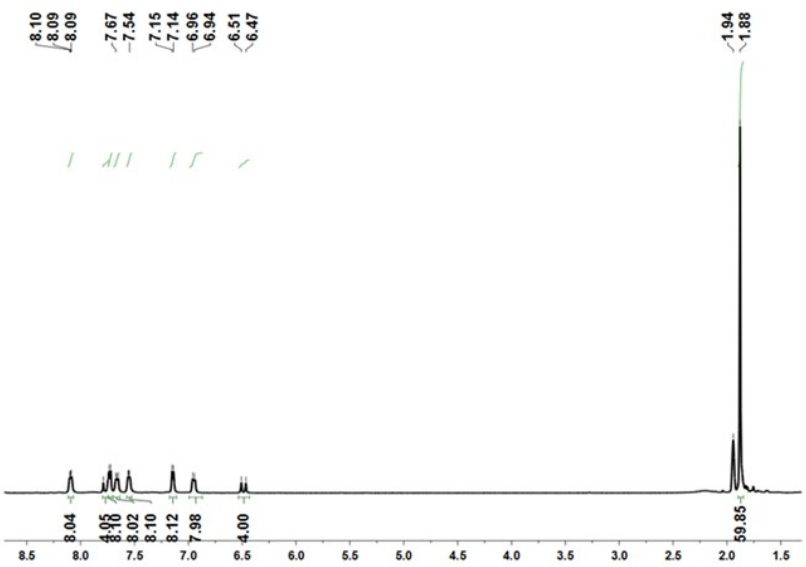

Figure S8. ^{1}H NMR (400 MHz, CD_3CN, ppm) of complex **5**.

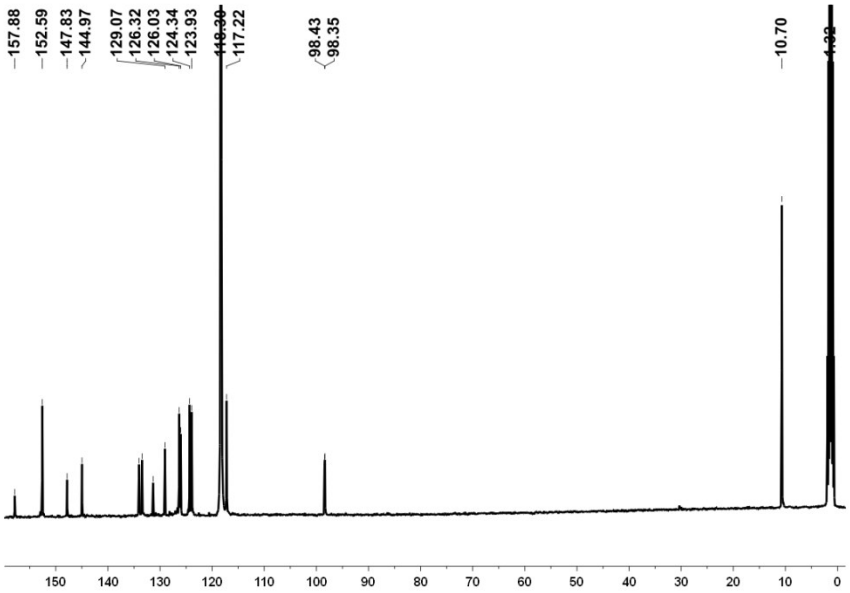

Figure S9. $^{13}C\{^{1}H\}$ NMR (101 MHz, CD_3CN, ppm) for complex **5**.

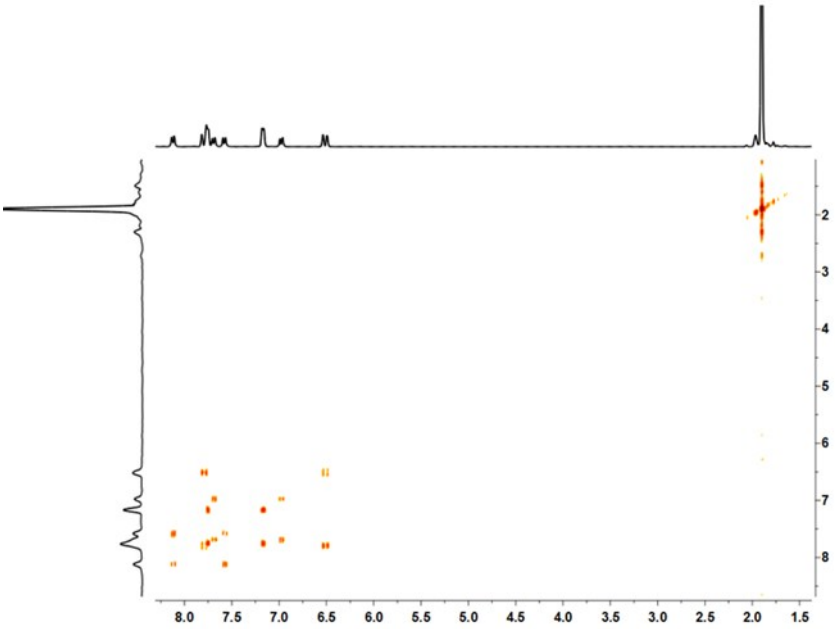

Figure S10. ^{1}H-^{1}H COSY NMR (400 MHz, CD_3CN, ppm) for complex **5**.

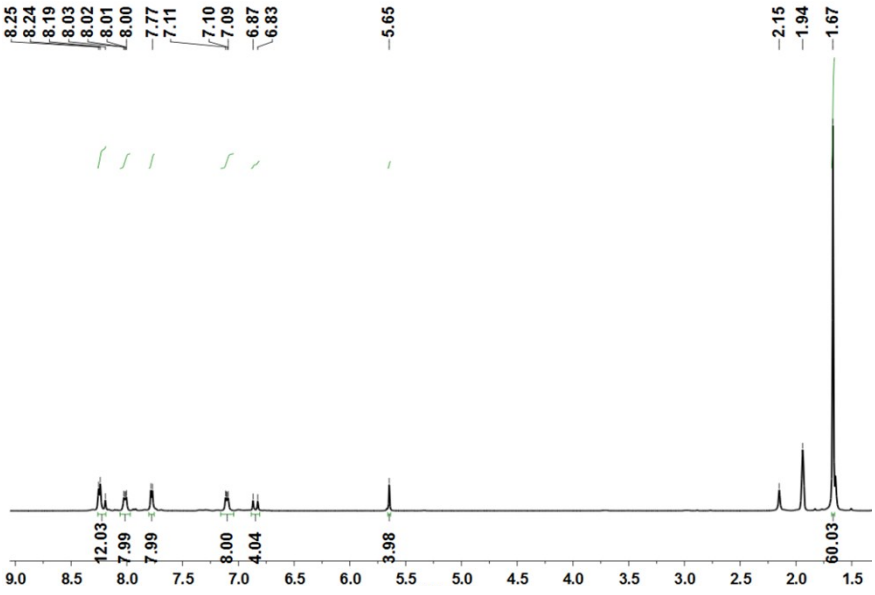

Figure S11. ^{1}H NMR (400 MHz, CD_3CN, ppm) for complex **6**.

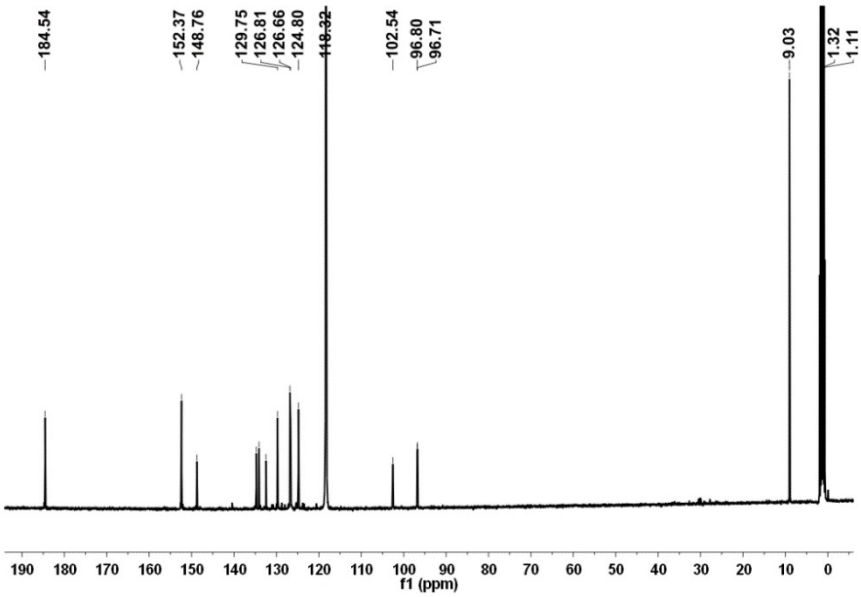

Figure S12. $^{13}C\{^{1}H\}$ NMR (101 MHz, CD_3CN, ppm) for complex **6**.

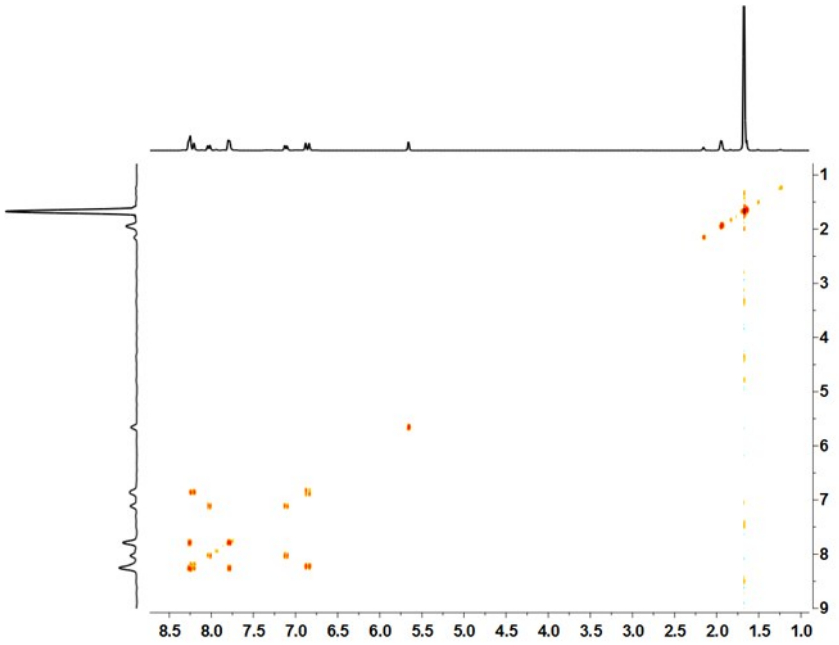

Figure S13. ^{1}H-^{1}H COSY NMR (400 MHz, CD_3CN, ppm) for complex **6**.

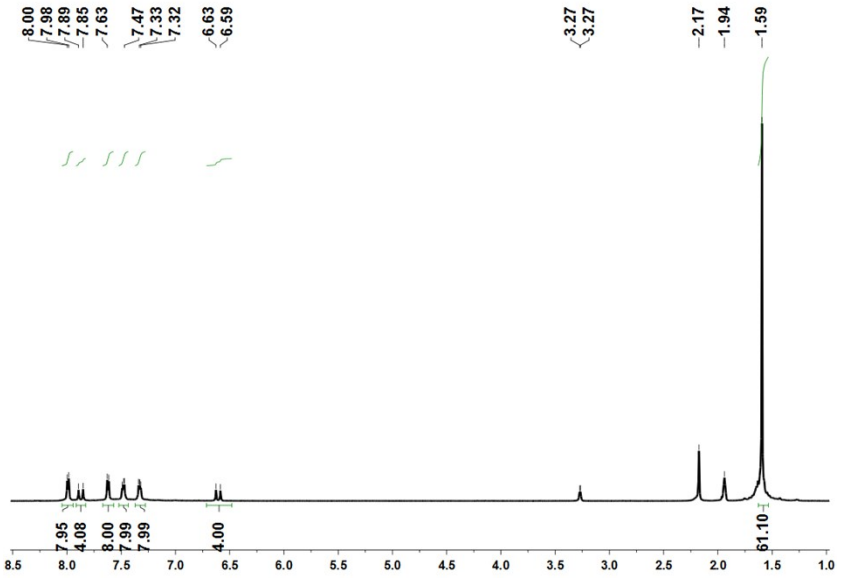

Figure S14. ^{1}H NMR (400 MHz, CD_3CN, ppm) for complex **4-O_2**.

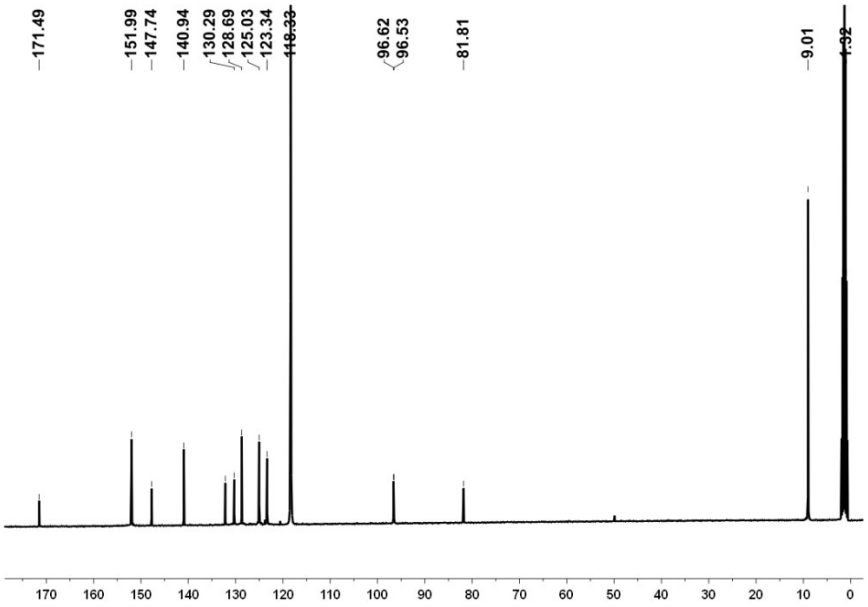

Figure S15. $^{13}C\{^{1}H\}$ NMR (101 MHz, CD_3CN, ppm) for complex **4-O_2**.

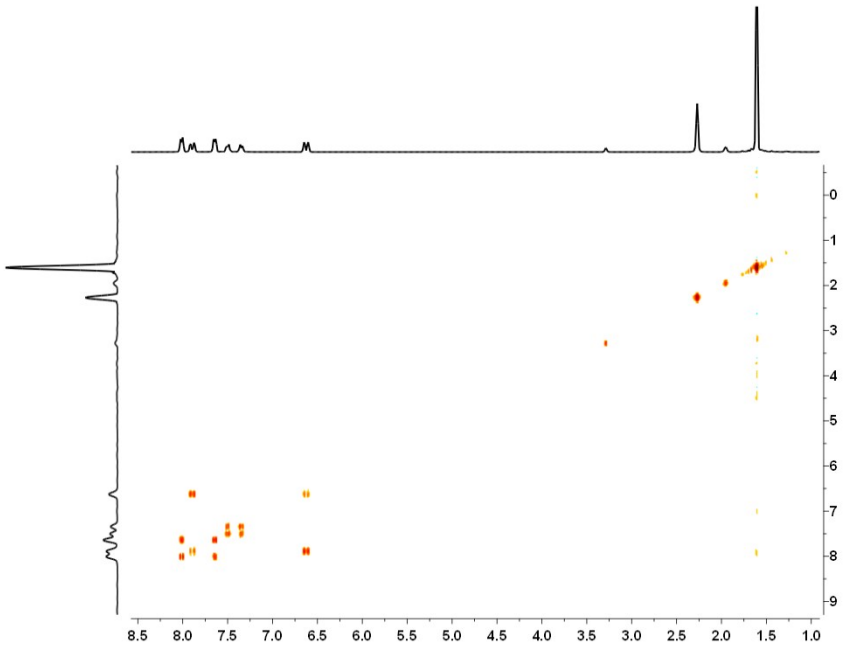

Figure S16. ^{1}H-^{1}H COSY NMR (400 MHz, CD_3CN, ppm) for complex **4-O$_2$**.

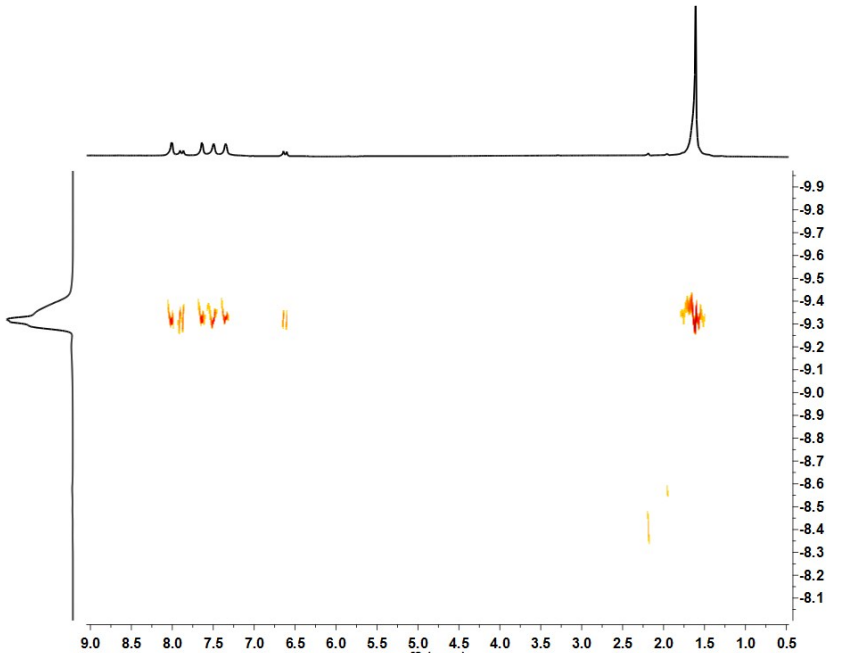

Figure S17. ^{1}H DOSY NMR (400 MHz, CD_3CN, ppm) for **4-O2**.

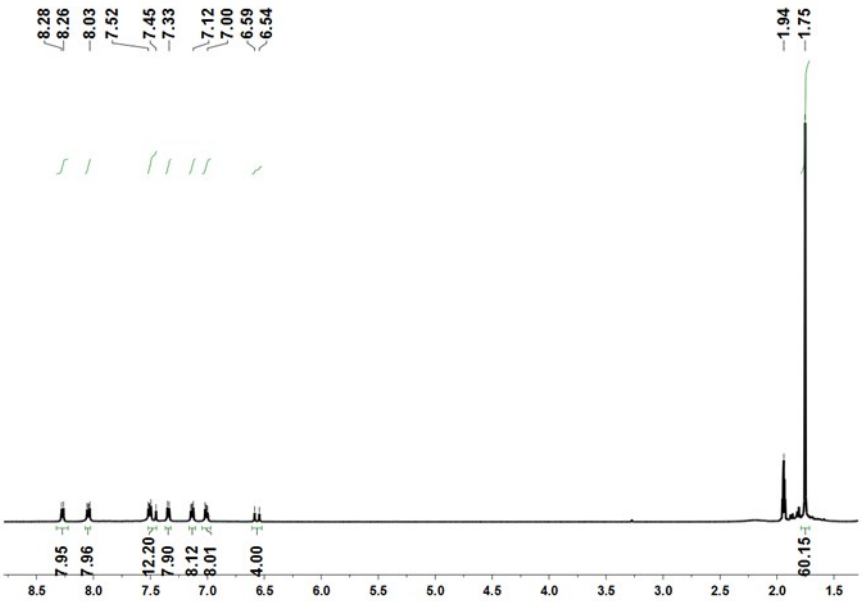

Figure S18. ^{1}H NMR (400 MHz, CD_3CN, ppm) for complex **5-O_2**.

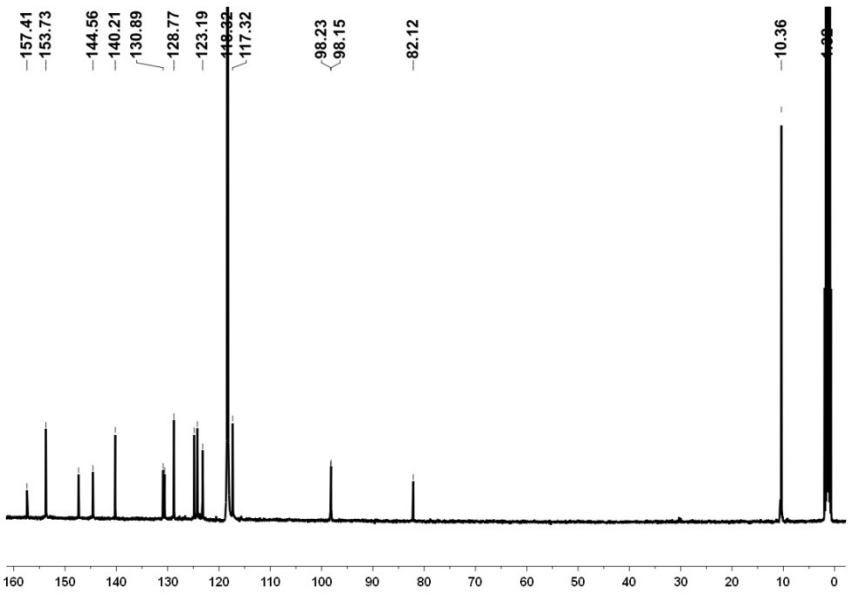

Figure S19. $^{13}C\{^{1}H\}$ NMR (101 MHz, CD_3CN, ppm) for complex **5-O_2**.

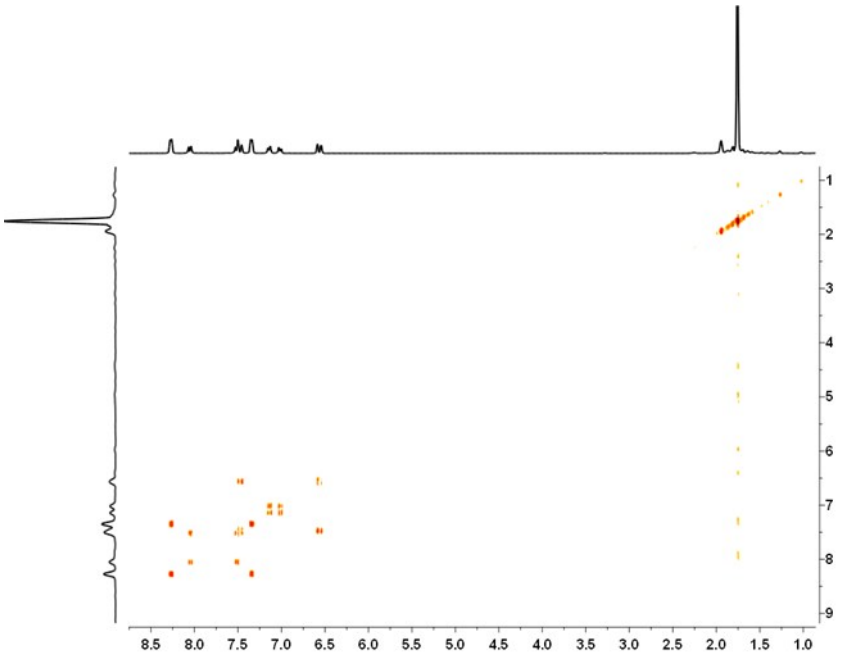

Figure S20. ^{1}H-^{1}H COSY NMR (400 MHz, CD_3CN, ppm) for complex **5-O$_2$**.

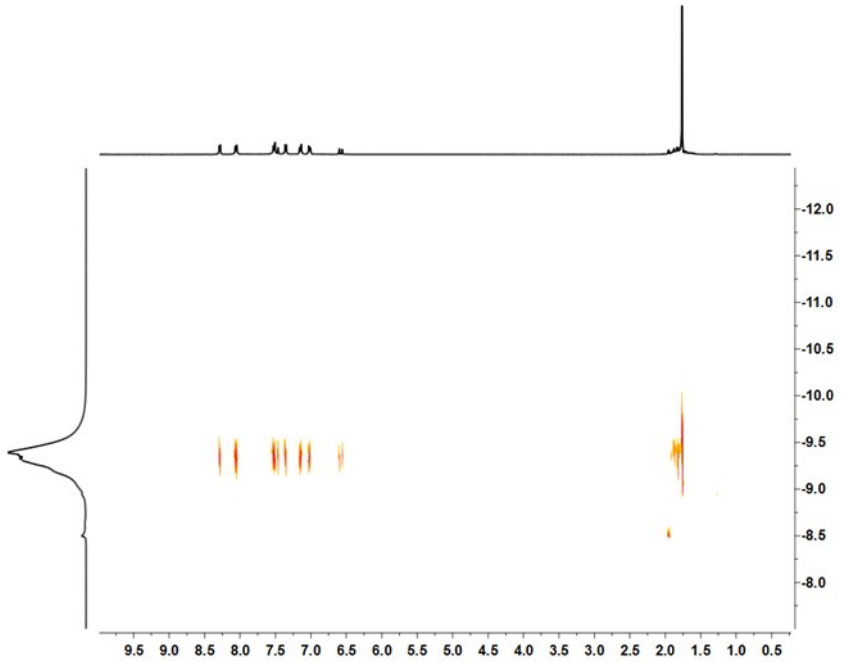

Figure S21.^{1}H DOSY NMR (400 MHz, CD_3CN, ppm) for complex **5-O$_2$**.

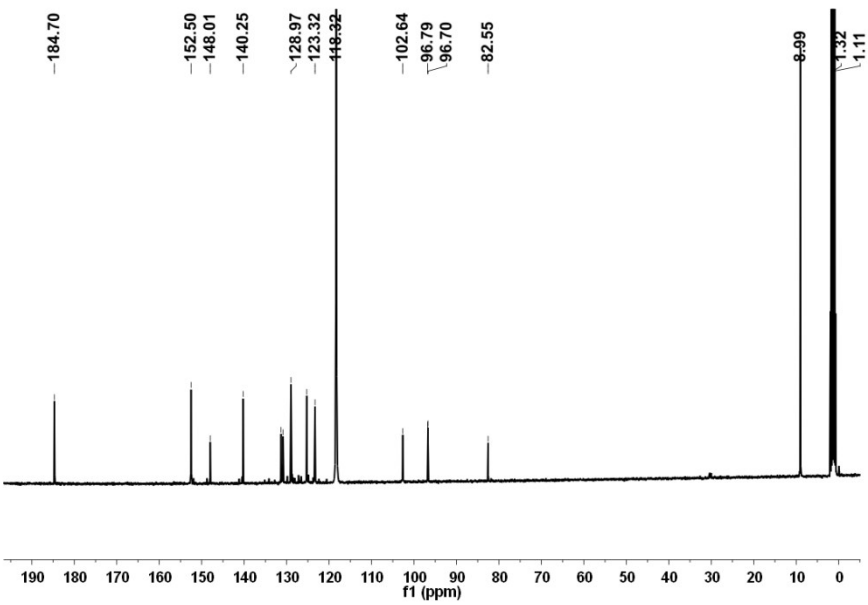

Figure S22. ^{1}H NMR (400 MHz, CD_3CN, ppm) for complex **6-O_2**.

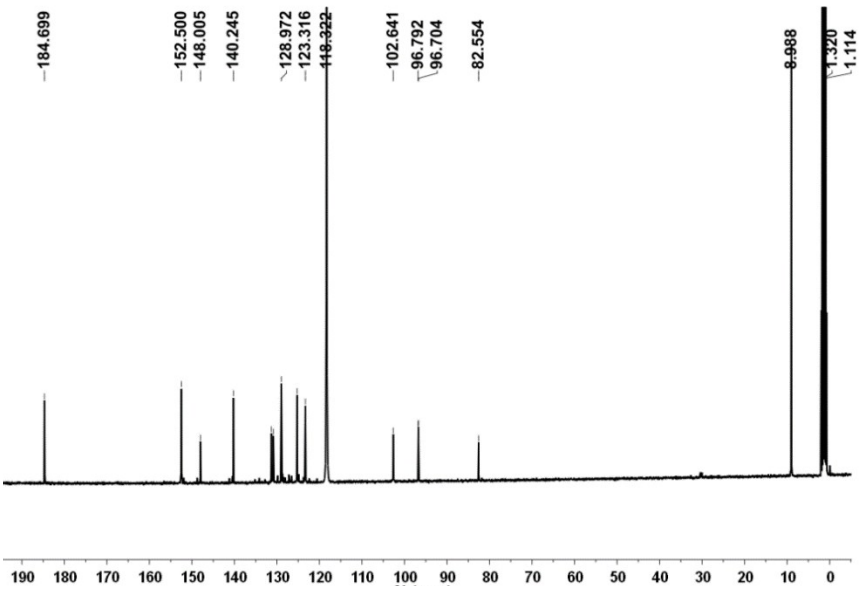

Figure S23. $^{13}C\{^{1}H\}$ NMR (101 MHz, CD_3CN, ppm) for complex **6-O_2**.

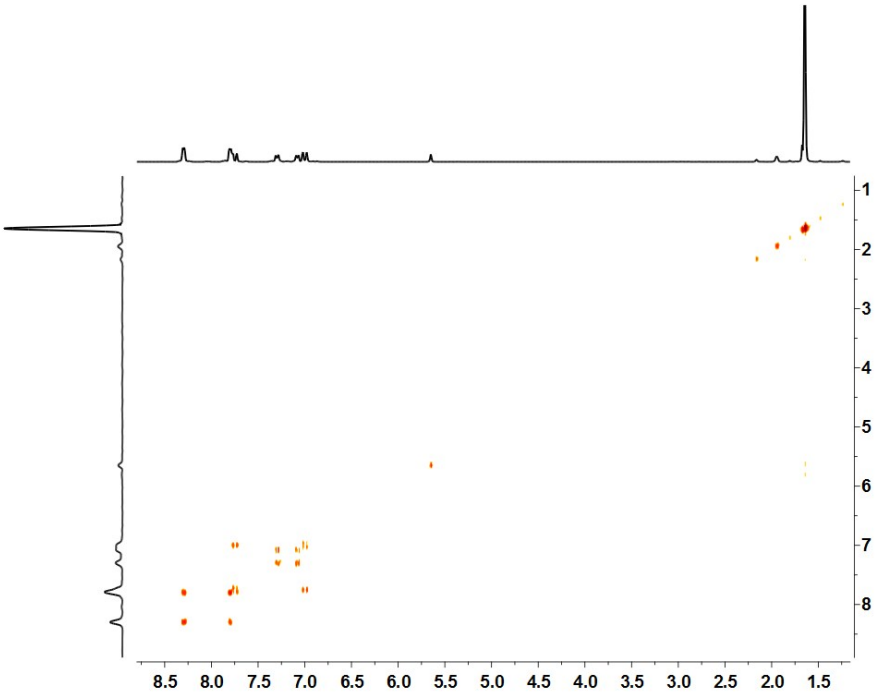

Figure S24. ^{1}H-^{1}H COSY NMR (400 MHz, CD_3CN, ppm) for complex **6-O$_2$**.

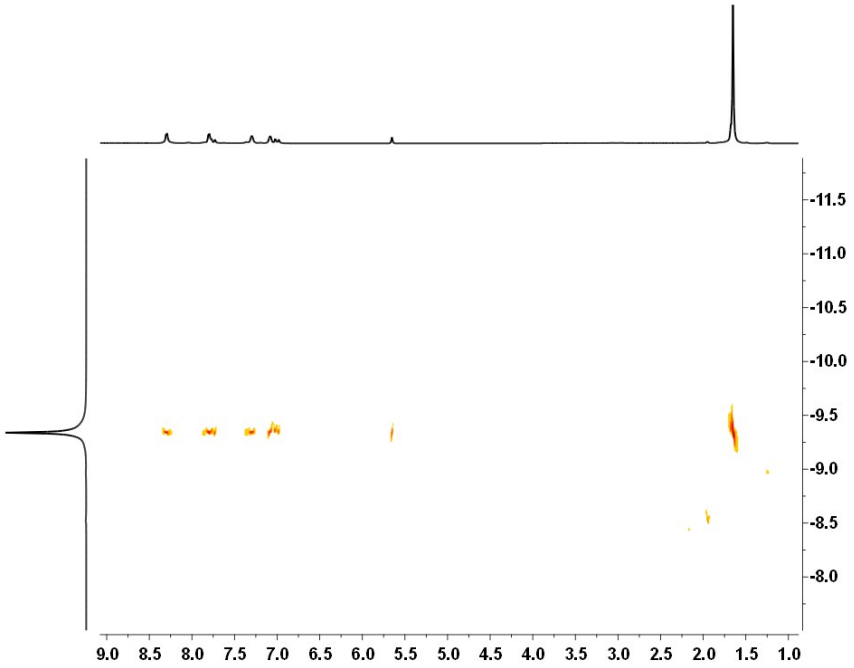

Figure S25. ^{1}H DOSY NMR (400 MHz, CD_3CN, ppm) for **6-O$_2$**.

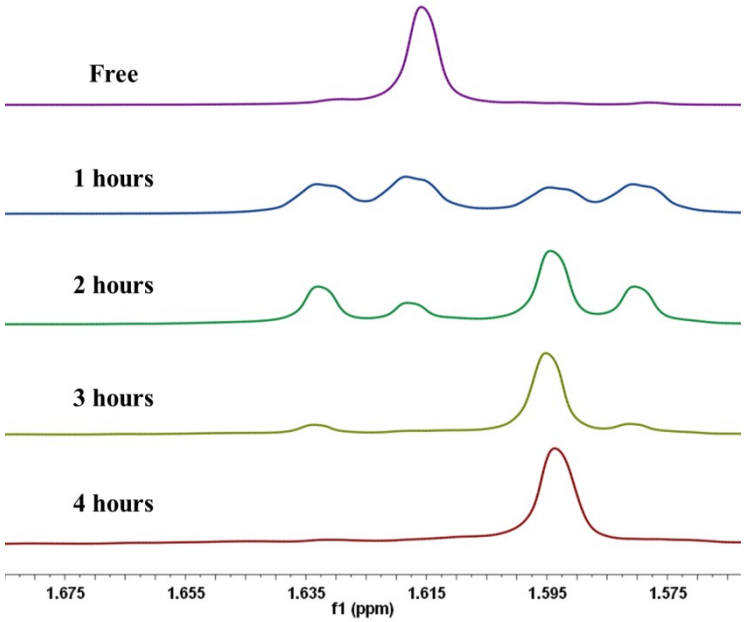

Figure S26. ^{1}H NMR (CD_3CN, 400 MHz, 25 °C) spectra of the Cp* signals of **4**; after irradiation at λ = 365 nm under air (free, 1h, 2h, 3h, and 4h).

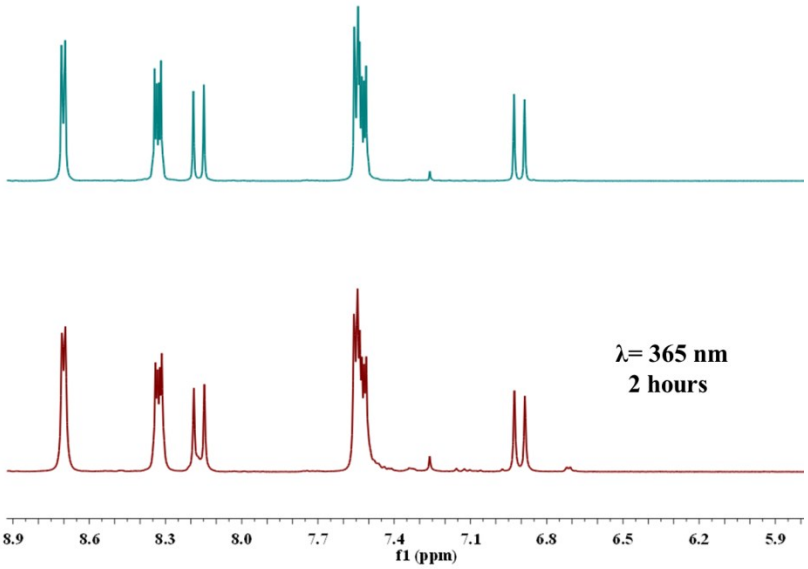

Figure S27. ^{1}H NMR ($CDCl_3$, 400 MHz, 25 °C) spectra of a 1 mM solution of **BP4VA** ligand; after irradiation at λ = 365 nm (2 h) under air.

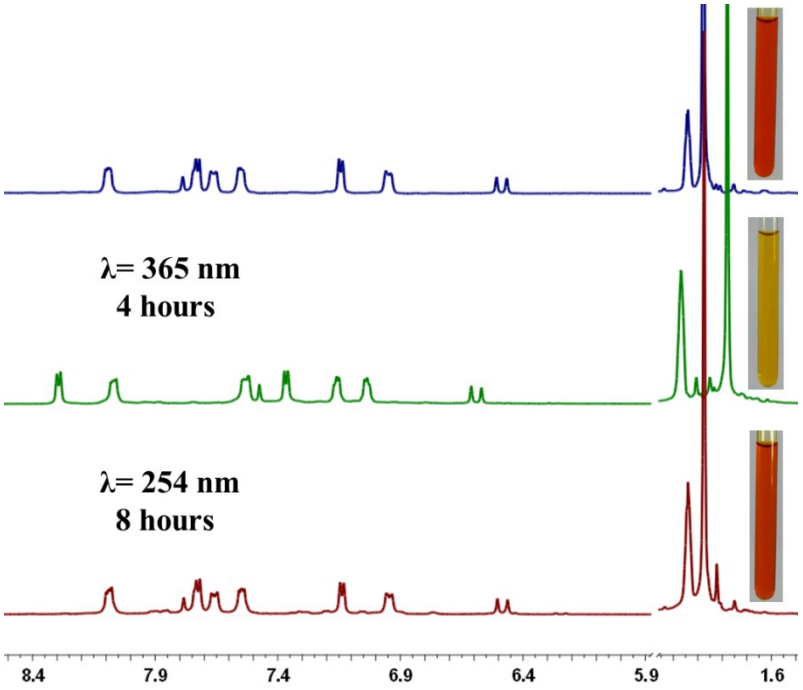

Figure S28. ^{1}H NMR (CD_3CN, 400 MHz, 25 °C) spectra of a 1 mM solution of **5**; after irradiation at λ = 365 nm (4 h) and irradiation at λ = 254 nm (8 h) under air.

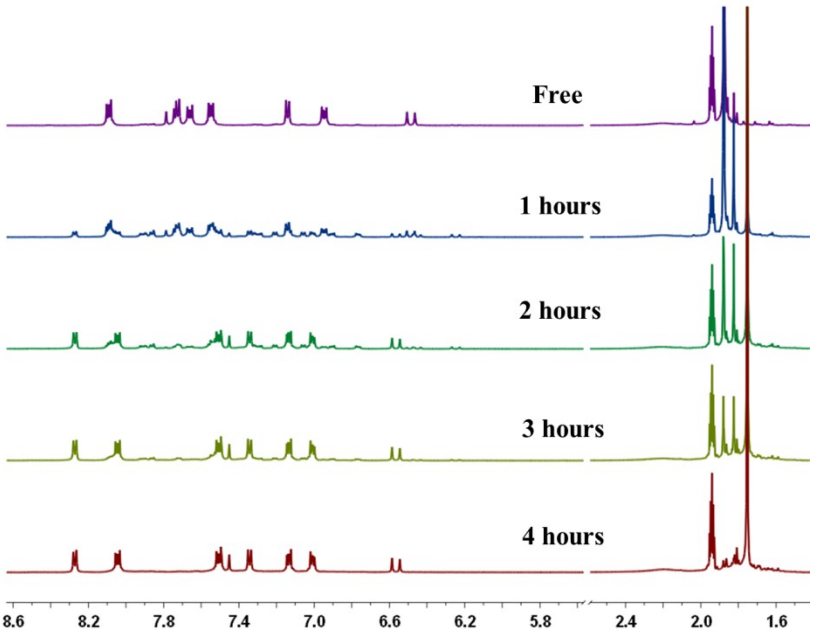

Figure S29. ^{1}H NMR (CD_3CN, 400 MHz, 25 °C) spectra of a 1 M solution of **5**; after irradiation at λ = 365 nm under air (free, 1h, 2h, 3h, and 4h).

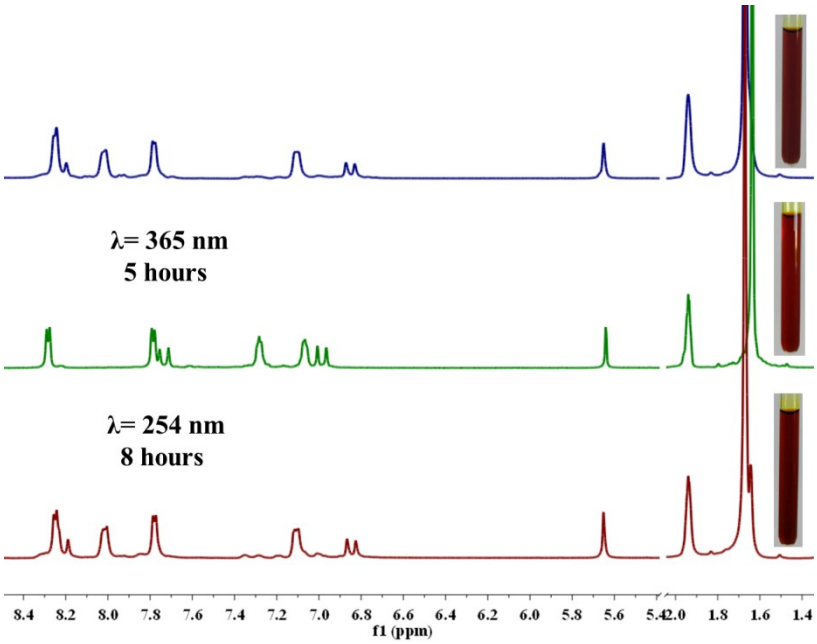

Figure S30. ^{1}H NMR (CD_3CN, 400 MHz, 25 °C) spectra of a 1 mM solution of **6**; after irradiation at λ = 365 nm (5 h) and irradiation at λ = 254 nm (8 h) under air.

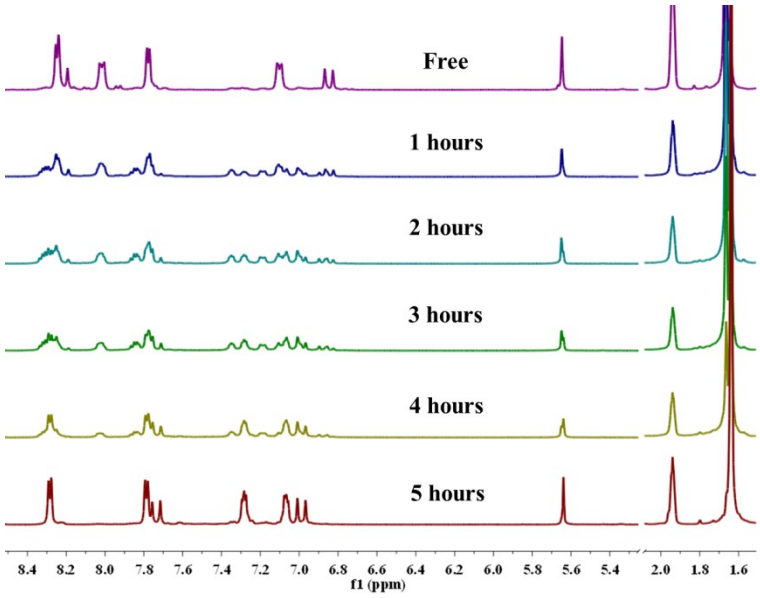

Figure S31. ^{1}H NMR (CD_3CN, 400 MHz, 25 °C) spectra of a 1 M solution of **6**; after irradiation at λ = 365 nm under air (free, 1h, 2h, 3h, 4h, and 5 h).

4. UV-vis spectroscopy

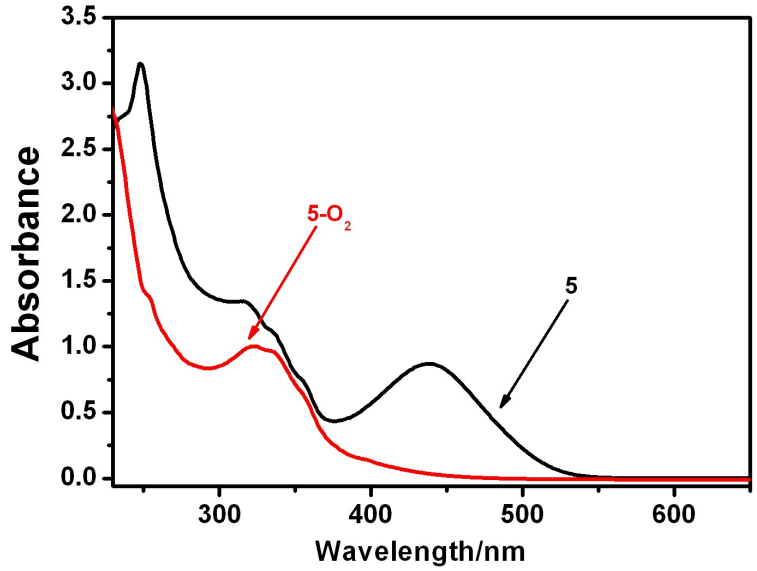

Figure S32. UV/vis spectra of a 1×10^{-5} M solution of **5** and **5-O_2** in CH_3CN.

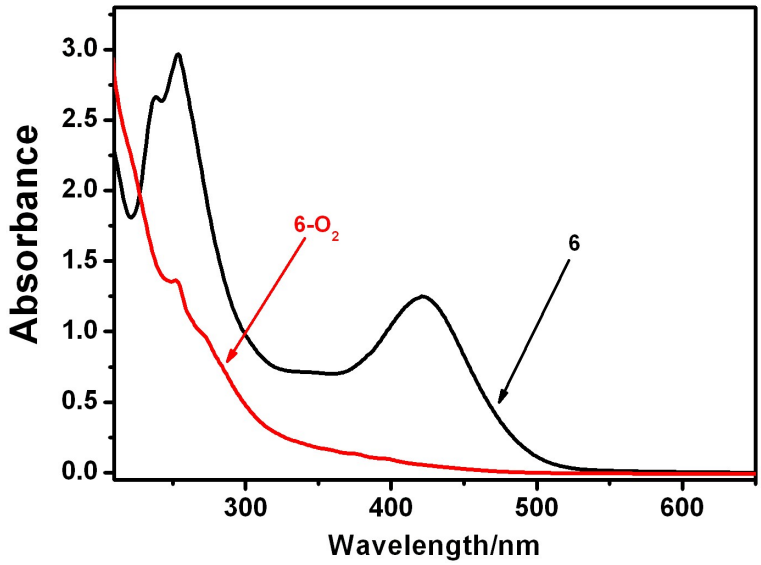

Figure S33. UV/vis spectra of a 1×10^{-5} M solution of **6** and **6-O_2** in CH_3CN.

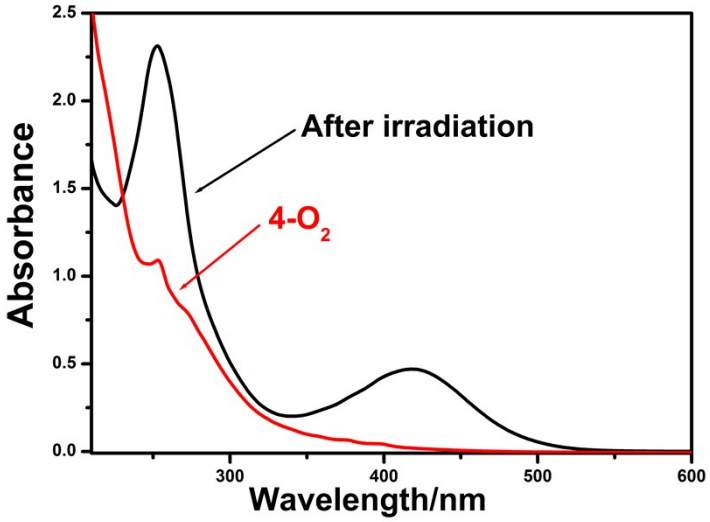

Figure S34. UV/vis spectra of a 1×10^{-5} M solution of **4** in CH_3CN was irradiated at $\lambda = 254$ nm.

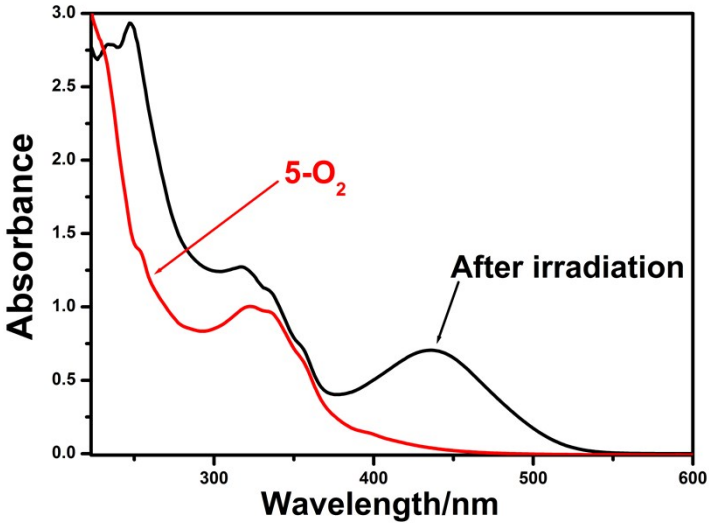

Figure S34. UV/vis spectra of a 1×10^{-5} M solution of **5** in CH_3CN was irradiated at $\lambda = 254$ nm.

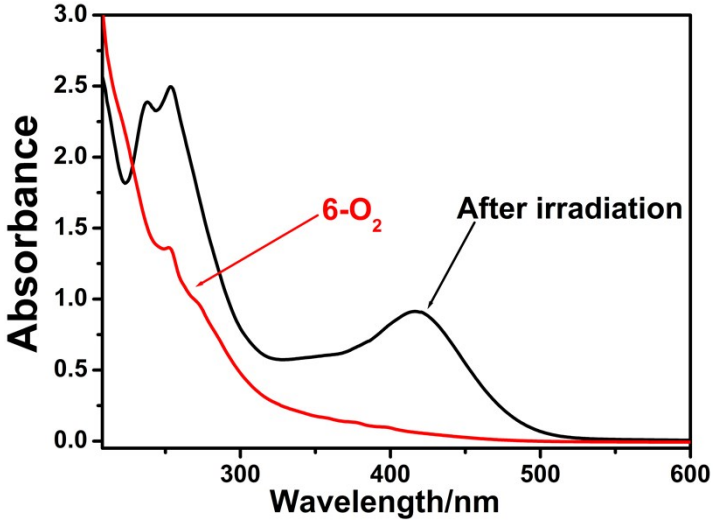

Figure S35. UV/vis spectra of a 1×10^{-5} M solution of **6** in CH_3CN was irradiated at $\lambda = 254$ nm.

5. X-ray crystallography details.

In asymmetric unit of **4**, there were disordered anion and solvents (one triflate anion, three methanol and one water molecules) which could not be restrained properly. Therefore, SQUEEZE algorithm was used to omit them. One bipyridine ligand and one triflate anion were disordered and they were divided into two parts (53:47 for bipyridine ligand and 60:40 for anion). 47 ISOR, 1 SIMU and 42 DFIX instructions were used to restrain anions, ligands and Cp* fragments so that there were 342 restraints in the data. Hydrogen of methanol molecule could not be found and others were put in calculated positions.

In asymmetric unit of **5**, there were disordered solvents (five acetonitrile molecules) which could not be restrained properly. Therefore, SQUEEZE algorithm was used to omit them. 32 ISOR and 18 DFIX instructions were used to restrain anions, solvents and Cp* fragments so that there were 210 restraints in the data.

In asymmetric unit of **6**, there were disordered anion and solvents (one triflate anion, three methanol and one water molecules) which could not be restrained properly. Therefore, SQUEEZE algorithm was used to omit them. The bipyridine ligand was disordered and it was divided into two parts (72:28). O8 was refined isotropically and other non-hydrogen atoms were refined anisotropically. 16 ISOR, 2 SIMU and 3 DFIX instructions were used to restrain disordered ligand so that there were 177 restraints in the data.

In asymmetric unit of **4-O_2**, there were disordered anions and solvents (two triflate anion and six water molecules) which could not be restrained properly. Therefore, SQUEEZE algorithm was used to omit them.

In asymmetric unit of **5-O_2**, there were disordered anion and solvents (one triflate anion, one methanol and one diethyl ether molecules) which could not be restrained properly. Therefore, SQUEEZE algorithm was used to omit them. One pentamethylcyclopentadienyl ligand was disordered and it was divided into two parts (60:40). 18 ISOR instructions were used to restrain disordered Cp* fragments so that there were 108 restraints in the data. Hydrogen of water molecules could not be found and others were put in calculated positions.

In asymmetric unit of **6-O_2**, there were disordered solvents (three acetonitrile molecules) which could not be restrained properly. Therefore, SQUEEZE algorithm was used to omit them. One triflate anion was disordered and it was divided into two parts (48:52). F8 was refined isotropically and other non-hydrogen atoms were refined anisotropically. 19 ISOR, 1 SIMU and 24 DFIX instructions were used to restrain anions, solvents and Cp* fragments so that there were 204 restraints in the data.

Table 1. Crystal data and structure refinement for **4**.

Empirical formula	C108 H118 F12 N4 O25 Rh4 S4	
Formula weight	2639.94	
Temperature	173(2) K	
Wavelength	1.54178 Å	
Crystal system	Triclinic	
Space group	P-1	
Unit cell dimensions	a = 17.0567(6) Å	α= 105.9447(19)°.
	b = 17.0598(7) Å	β= 111.7756(16)°.
	c = 22.6028(8) Å	γ= 94.6228(18)°.
Volume	5748.8(4) $Å^3$	
Z	2	
Density (calculated)	1.525 Mg/m^3	
Absorption coefficient	6.023 mm^{-1}	
F(000)	2692	
Crystal size	0.250 x 0.220 x 0.180 mm^3	
Theta range for data collection	2.229 to 68.999°.	
Index ranges	-20<=h<=20, -20<=k<=20, -27<=l<=27	
Reflections collected	66858	
Independent reflections	20637 [R(int) = 0.0575]	
Completeness to theta = 67.679°	96.6 %	
Absorption correction	Semi-empirical from equivalents	
Max. and min. transmission	0.754 and 0.494	
Refinement method	Full-matrix least-squares on F^2	
Data / restraints / parameters	20637 / 342 / 1421	
Goodness-of-fit on F^2	1.041	
Final R indices [I>2sigma(I)]	R1 = 0.0810, wR2 = 0.2286	
R indices (all data)	R1 = 0.0947, wR2 = 0.2406	
Extinction coefficient	n/a	
Largest diff. peak and hole	2.583 and -1.302 e.$Å^{-3}$	

$aR_1 = \Sigma||F_o| - |F_c||$ (based on reflections with $Fo^2 > 2\sigma F^2$); $wR_2 = \{\Sigma[\omega(Fo^2 - Fc^2)^2]/\Sigma[\omega(Fo^2)^2]\}^{1/2}$; $w = 1/[\sigma^2 F_0^2 + (0.095P)^2]$; $P = [\max(Fo^2, 0) + 2Fc^2]/3$ (also with $Fo^2 > 2\sigma F^2$).

Table 2. Crystal data and structure refinement for **5**.

Empirical formula	C150 H157 F12 N19 O14 Rh4 S4	
Formula weight	3217.82	
Temperature	202(2) K	
Wavelength	0.71073 Å	
Crystal system	Triclinic	
Space group	P-1	
Unit cell dimensions	a = 13.3420(15) Å	α= 95.573(2)°.
	b = 22.628(3) Å	β= 90.823(2)°.
	c = 25.834(3) Å	γ= 104.286(2)°.
Volume	7516.5(15) $Å^3$	
Z	2	
Density (calculated)	1.422 Mg/m^3	
Absorption coefficient	0.568 mm^{-1}	
F(000)	3308	
Crystal size	0.240 x 0.230 x 0.210 mm^3	
Theta range for data collection	0.793 to 25.249°.	
Index ranges	-16<=h<=14, -27<=k<=26, -31<=l<=24	
Reflections collected	43484	
Independent reflections	26819 [R(int) = 0.0568]	
Completeness to theta = 25.242°	98.7 %	
Absorption correction	Semi-empirical from equivalents	
Max. and min. transmission	0.684 and 0.497	
Refinement method	Full-matrix least-squares on F^2	
Data / restraints / parameters	26819 / 210 / 1717	
Goodness-of-fit on F^2	0.966	
Final R indices [I>2sigma(I)]	R1 = 0.0971, wR2 = 0.2623	
R indices (all data)	R1 = 0.1572, wR2 = 0.3192	
Extinction coefficient	n/a	
Largest diff. peak and hole	2.043 and -2.070 $e.Å^{-3}$	

$aR_1 = \Sigma||F_o| - |F_c||$ (based on reflections with $Fo^2 > 2\sigma F^2$); $wR_2 = \{\Sigma[\omega(Fo^2 - Fc^2)^2]/\Sigma[\omega(Fo^2)^2]\}^{1/2}$; $w = 1/[\sigma^2 F_0^2 + (0.095P)^2]$; $P = [\max(Fo^2, 0) + 2Fc^2]/3$ (also with $Fo^2 > 2\sigma F^2$).

Table 3. Crystal data and structure refinement for **6**.

Empirical formula	C118 H132 F12 N4 O28 Rh4 S4	
Formula weight	2822.15	
Temperature	173(2) K	
Wavelength	1.54178 Å	
Crystal system	Monoclinic	
Space group	$P2_1/n$	
Unit cell dimensions	a = 18.2667(5) Å	α= 90°.
	b = 13.9397(4) Å	β= 100.7940(10)°.
	c = 24.7859(6) Å	γ= 90°.
Volume	6199.6(3) $Å^3$	
Z	2	
Density (calculated)	1.512 Mg/m^3	
Absorption coefficient	5.644 mm^{-1}	
F(000)	2888	
Crystal size	0.440 x 0.320 x 0.070 mm^3	
Theta range for data collection	3.322 to 67.999°.	
Index ranges	-21<=h<=21, -16<=k<=14, -27<=l<=29	
Reflections collected	37173	
Independent reflections	10929 [R(int) = 0.0500]	
Completeness to theta = 67.679°	96.9 %	
Absorption correction	Semi-empirical from equivalents	
Max. and min. transmission	0.424 and 0.263	
Refinement method	Full-matrix least-squares on F^2	
Data / restraints / parameters	10929 / 177 / 703	
Goodness-of-fit on F^2	0.880	
Final R indices [I>2sigma(I)]	R1 = 0.0613, wR2 = 0.1667	
R indices (all data)	R1 = 0.0771, wR2 = 0.1863	
Extinction coefficient	n/a	
Largest diff. peak and hole	1.982 and -0.554 e.$Å^{-3}$	

$aR_1 = \Sigma||F_o| - |F_c||$ (based on reflections with $Fo^2 > 2\sigma F^2$); $wR_2 = \{\Sigma[\omega(Fo^2 - Fc^2)^2]/\Sigma[\omega(Fo^2)^2]\}^{1/2}$; $w = 1/[\sigma^2 F_0^2 + (0.095P)^2]$; $P = [\max(Fo^2, 0) + 2Fc^2]/3$ (also with $Fo^2 > 2\sigma F^2$).

Table 4. Crystal data and structure refinement for **4-O_2**.

Empirical formula	C128 H100 F12 N4 O36 Rh4 S4	
Formula weight	3037.99	
Temperature	173(2) K	
Wavelength	1.54178 Å	
Crystal system	Monoclinic	
Space group	C2/c	
Unit cell dimensions	a = 37.892(4) Å	α= 90°.
	b = 16.2390(15) Å	β= 130.389(5)°.
	c = 27.209(5) Å	γ= 90°.
Volume	12752(3) $Å^3$	
Z	4	
Density (calculated)	1.582 Mg/m^3	
Absorption coefficient	5.592 mm^{-1}	
F(000)	6144	
Crystal size	0.350 x 0.240 x 0.090 mm^3	
Theta range for data collection	3.122 to 70.533°.	
Index ranges	-45<=h<=25, -19<=k<=18, -30<=l<=33	
Reflections collected	33179	
Independent reflections	11959 [R(int) = 0.0744]	
Completeness to theta = 67.679°	99.5 %	
Absorption correction	Semi-empirical from equivalents	
Max. and min. transmission	0.322 and 0.179	
Refinement method	Full-matrix least-squares on F^2	
Data / restraints / parameters	11959 / 0 / 551	
Goodness-of-fit on F^2	1.089	
Final R indices [I>2sigma(I)]	R1 = 0.1175, wR2 = 0.3393	
R indices (all data)	R1 = 0.1968, wR2 = 0.3932	
Extinction coefficient	n/a	
Largest diff. peak and hole	2.018 and -0.544 $e.Å^{-3}$	

$aR_1 = \Sigma||F_o| - |F_c||$ (based on reflections with $Fo^2 > 2\sigma F^2$); $wR_2 = \{\Sigma[\omega(Fo^2 - Fc^2)^2]/\Sigma[\omega(Fo^2)^2]\}^{1/2}$; $w = 1/[\sigma^2 F_0^2 + (0.095P)^2]$; $P = [\max(Fo^2, 0) + 2Fc^2]/3$ (also with $Fo^2 > 2\sigma F^2$).

Table 5. Crystal data and structure refinement for **5-O_2**.

Empirical formula	C138 H152 F12 N12 O24 Rh4 S4	
Formula weight	3130.59	
Temperature	173(2) K	
Wavelength	1.54178 Å	
Crystal system	Monoclinic	
Space group	C2/c	
Unit cell dimensions	a = 42.7915(8) Å	α= 90°.
	b = 13.9984(3) Å	β= 99.1800(9)°.
	c = 24.5974(4) Å	γ= 90°.
Volume	14545.4(5) $Å^3$	
Z	4	
Density (calculated)	1.430 Mg/m^3	
Absorption coefficient	4.866 mm^{-1}	
F(000)	6432	
Crystal size	0.250 x 0.220 x 0.180 mm^3	
Theta range for data collection	2.092 to 72.546°.	
Index ranges	-52<=h<=49, -16<=k<=17, -30<=l<=29	
Reflections collected	43998	
Independent reflections	14227 [R(int) = 0.0694]	
Completeness to theta = 67.679°	99.5 %	
Absorption correction	Semi-empirical from equivalents	
Max. and min. transmission	0.754 and 0.577	
Refinement method	Full-matrix least-squares on F^2	
Data / restraints / parameters	14227 / 108 / 798	
Goodness-of-fit on F^2	1.063	
Final R indices [I>2sigma(I)]	R1 = 0.0711, wR2 = 0.1999	
R indices (all data)	R1 = 0.1000, wR2 = 0.2203	
Extinction coefficient	n/a	
Largest diff. peak and hole	3.233 and -1.619 e.$Å^{-3}$	

$aR_1 = \Sigma||F_o| - |F_c||$ (based on reflections with $Fo^2 > 2\sigma F^2$); $wR_2 = \{\Sigma[\omega(Fo^2 - Fc^2)^2]/\Sigma[\omega(Fo^2)^2]\}^{1/2}$; $w = 1/[\sigma^2 F_0^2 + (0.095P)^2]$; $P = [\max(Fo^2, 0) + 2Fc^2]/3$ (also with $Fo^2 > 2\sigma F^2$).

Table 6. Crystal data and structure refinement for **6-O_2**.

Empirical formula	C136 H148 F12 N12 O26 Rh4 S4	
Formula weight	3134.54	
Temperature	173(2) K	
Wavelength	0.71073 Å	
Crystal system	Monoclinic	
Space group	$P2_1/c$	
Unit cell dimensions	a = 21.637(3) Å	α= 90°.
	b = 14.6321(17) Å	β= 100.052(2)°.
	c = 23.470(3) Å	γ= 90°.
Volume	7316.4(14) $Å^3$	
Z	2	
Density (calculated)	1.423 Mg/m^3	
Absorption coefficient	0.586 mm^{-1}	
F(000)	3216	
Crystal size	0.410 x 0.310 x 0.250 mm^3	
Theta range for data collection	0.956 to 26.949°.	
Index ranges	-27<=h<=27, -18<=k<=17, -29<=l<=26	
Reflections collected	49258	
Independent reflections	15657 [R(int) = 0.0675]	
Completeness to theta = 25.242°	99.5 %	
Absorption correction	Semi-empirical from equivalents	
Max. and min. transmission	0.745 and 0.618	
Refinement method	Full-matrix least-squares on F^2	
Data / restraints / parameters	15657 / 204 / 874	
Goodness-of-fit on F^2	1.008	
Final R indices [I>2sigma(I)]	R1 = 0.0799, wR2 = 0.2271	
R indices (all data)	R1 = 0.1230, wR2 = 0.2558	
Extinction coefficient	n/a	
Largest diff. peak and hole	4.207 and -1.687 e.$Å^{-3}$	

$aR_1 = \Sigma||F_o| - |F_c||$ (based on reflections with $Fo^2 > 2\sigma F^2$); $wR_2 = \{\Sigma[\omega(Fo^2 - Fc^2)^2]/\Sigma[\omega(Fo^2)^2]\}^{1/2}$; $w = 1/[\sigma^2 F_0^2 + (0.095P)^2]$; $P = [\max(Fo^2, 0) + 2Fc^2]/3$ (also with $Fo^2 > 2\sigma F^2$).